Structure determination of the $(\sqrt{3}\times\sqrt{3})R30°$ boron phase on the Si(111) surface using photoelectron diffraction

P. Baumgärtel, J. J. Paggel, M. Hasselblatt, K. Horn, V. Fernandez, O. Schaff, J. H. Weaver,* and A. M. Bradshaw
Fritz-Haber-Institut der Max-Planck-Gesellschaft, Faradayweg 4-6, 14195 Berlin-Dahlem, Germany

D. P. Woodruff
Department of Physics, University of Warwick, Coventry CV4 7AL, United Kingdom

E. Rotenberg
Advanced Light Source, MS2-400, Lawrence Berkeley National Laboratory, Berkeley, California 94720

J. Denlinger
Physics Department, University of Wisconsin-Milwaukee, 1900 E. Kenwood Boulevard, Milwaukee, Wisconsin 53211
(Received 19 November 1998)

A quantitative structural analysis of the system Si(111)$(\sqrt{3}\times\sqrt{3})R30°$-B has been performed using photoelectron diffraction in the scanned energy mode. We confirm that the substitutional S_5 adsorption site is occupied and show that the interatomic separations to the three nearest-neighbor Si atoms are $1.98(\pm 0.04)$ Å, $2.14(\pm 0.13)$ Å, and $2.21(\pm 0.12)$ Å. These correspond to the silicon atom immediately below the boron atom, the adatom immediately above, and the three atoms to which it is coordinated symmetrically in the first layer. [S0163-1829(99)05819-1]

I. INTRODUCTION

The Si(111)$(\sqrt{3}\times\sqrt{3})R30°$-B phase on Si(111) has been investigated extensively in the last ten years because of its unique structure and properties.[1–31] It is energetically the most stable phase formed by boron on the Si(111) surface. Quantitative structural studies using x-ray diffraction[1,2] and low-energy electron diffraction (LEED),[3] total-energy calculations[4,5] as well as scanning tunneling microscopy[6,7] have demonstrated that the boron atom occupies the substitutional (S_5) site directly below a silicon atom in a T_4 site, as shown in Fig. 1(a). The ideally truncated bulk structure is shown for comparison in Fig. 1(b). This geometry contrasts with that formed by the other Group III elements Al, Ga, and In where the adatoms are in the T_4 site. This is due to the fact that the latter have covalent radii which are larger than that of Si. The covalent radius of boron is smaller which would lead to B-Si bonds in the T_4 site much shorter than the substrate bonds, giving rise to considerable strain. Moreover, the short bond would place a boron atom in the T_4 site very close to the second layer Si atom situated beneath, leading to strong overlap repulsion.

The properties of the Si(111)$(\sqrt{3}\times\sqrt{3})R30°$-B structure appear to have their origin in the charge transfer between the boron and the silicon atom directly above. This gives rise to a substantially lower reactivity than on the clean Si(111)(7×7) surface,[8,9] as indicated by a range of adsorption experiments.[10–20] The phase is also stable with respect to the deposition of Si overlayers which opens up the possibility of producing ordered δ-doping.[2,21–27] Some effort has been directed towards characterizing the Si(111)$(\sqrt{3}\times\sqrt{3})R30°$-B phase. The assignment of surface core level shifts in photoemission measurements remains controversial,[19,28–30] however, despite comparison with *ab initio* pseudopotential calculations.[31] We are aware of only two experimental structural analyses in which geometrical parameters have been determined quantitatively. Headrick *et al.*[1] have employed grazing-incidence x-ray diffraction using synchrotron radiation, a technique which is not very sensitive to boron because of its low x-ray scattering factor thus leading to relatively poor precision with respect to its position. Indeed, in this study the location of the B atom is inferred largely through the absence of an expected Si atom, and the investigation then concentrated on determining the Si atom displacements produced by the B. A low scattering factor for elastic scattering of low-energy electrons also constrains the precision of the dynamical LEED study reported by Huang *et al.*,[3] although in this investigation specific B-Si near-neighbor distances were deduced.

In the present paper we report a scanned-energy mode photoelectron diffraction (PhD) study of this system. In previous papers we have shown that this technique provides detailed quantitative information on the local structure, especially on the adsorption site and adatom-substrate bond lengths.[32–36] The method exploits the interference between the directly emitted part of the photoelectron wave field from an adsorbate core level with those components of the wave field elastically scattered by surrounding atoms. This effect modulates the intensity of the adsorbate core-level photoelectron line in a particular emission direction when the photon energy, and thus the photoelectron kinetic energy, is varied. The modulations in turn depend on the contributing path length differences and thus provide the desired information on the local geometry of the emitter atom. In the present study B $1s$ photoelectron diffraction spectra have been measured; these provide quantitative information on the location

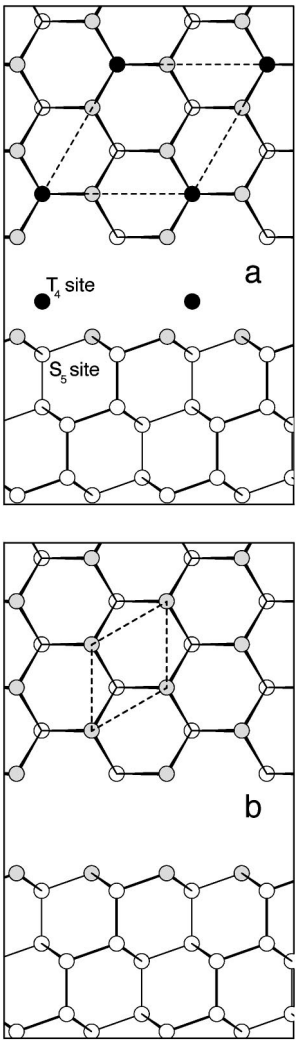

FIG. 1. (a) Plan and side views of a Si(111)$(\sqrt{3}\times\sqrt{3})R30°$ adsorption structure with the adsorbate atoms (black circles) in the T_4 sites. The Si atom in the second layer corresponding to the S_5 substitutional site is also labeled. The dashed lines show the $(\sqrt{3}\times\sqrt{3})R30°$ surface unit mesh. The grey circles denote outermost layer Si atoms. (b) Plan and side views of an ideally terminated bulk Si(111) surface, otherwise as in (a). The dashed lines show the (1×1) surface unit mesh.

of the B atom *shape which does not depend on weak scattering from the B atoms*. The challenging aspect of applying the PhD technique to this system lies in the low photoionization cross section of the B 1*s* state, but this has been overcome through the use of undulator radiation from the third-generation advanced light source (ALS). Our investigation allowed us to determine the structural parameters with a higher precision than in previous structural studies[1,2] and they are in close agreement with theory.[4,5]

II. EXPERIMENTAL DETAILS

The experiments were performed on beam line 7.0.1 at the ALS, at the Lawrence Berkeley National Laboratory, California. The 5-cm-period undulator has its third harmonic in the range 180–520 eV at a nominal electron beam energy of 1.9 GeV. The spherical grating monochromator and the layout of the beam line have been described by Warwick

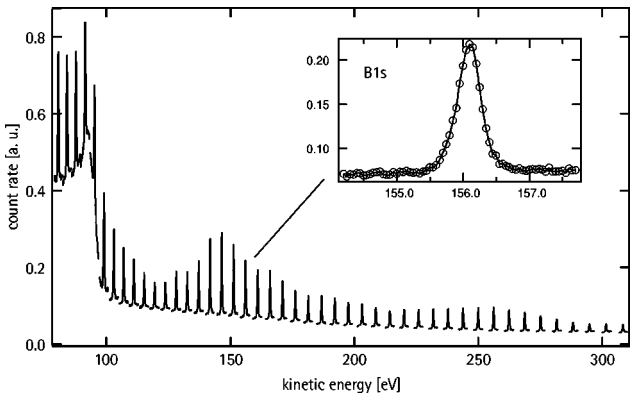

FIG. 2. ''Group plot'' of the raw data for the B 1*s* PhD spectrum recorded at normal emission, showing the individual B 1*s* energy distribution curves (EDC's) recorded at different photon energies. The inset shows one of these EDC's expanded.

et al.[37,38] A Perkin-Elmer Omni IV electron spectrometer with a mean radius of 137 mm accepts the emitted photoelectrons at an angle of 60° relative to the photon beam in the plane of incidence. The heavily doped Si(111) crystal wafer $(1\times10^{20}$ B cm$^{-3})$ was cleaned *in situ* by flashing to $\sim$1200° C. Subsequent, repeated short anneals to $\sim$900° C promoted the diffusion of boron to the surface and the appearance of a sharp Si(111)$(\sqrt{3}\times\sqrt{3})R30°$ LEED pattern. Photoelectron spectra were recorded for the B 1*s* core-level (electron binding energy $\sim$188 eV) in the kinetic energy range 80–320 eV at five polar angles (including normal emission) in two azimuthal directions at a sample temperature of 240 K.

The signal was recorded at successive photon energies (separated by a constant value of the photoelectron wave vector, $\vec{k}$), in a kinetic energy window of 3.5 eV around the B 1*s* core-level peak to give a series of energy distribution curves (EDC's). These are shown in Fig. 2 as a so-called group plot for the normal emission data set. The intensity of each peak was then determined by background subtraction and integration, and the resulting intensity-energy spectrum was normalized to give the modulation function defined by

$$\chi_{\mathrm{ex}}(\theta,\phi,k)=\frac{I(k)-I_0(k)}{I_0(k)}, \tag{1}$$

where I and I_0 are the diffractive and nondiffractive intensities and θ and ϕ are the polar and azimuthal emission angles. The resulting modulation functions for the five directions are shown as the bold curves in Fig. 3. In the case of the present data there was no overlap between energy windows at successive photon energies. In our previous experiments on a bending magnet beam line at the BESSY I electron storage ring this always proved necessary in order to ensure adequate background subtraction. The superior spectral resolution at the ALS leads to narrow peaks ($\sim$0.5 eV) for which a simple straight line background extrapolated from the high kinetic energy side of the spectra proves sufficient. The procedure even proves to be effective in the presence of intense background features such as the Si Auger emission at $\sim$90 eV in Fig. 2.

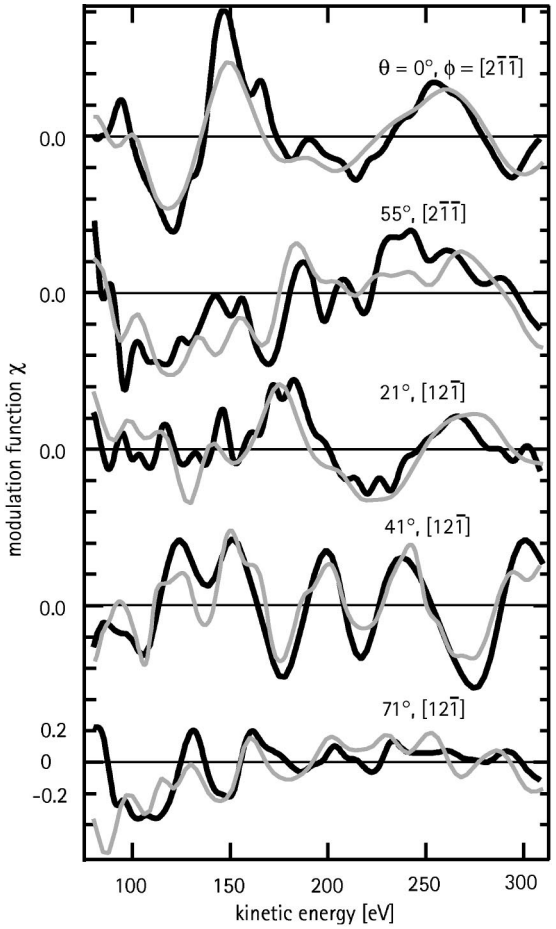

FIG. 3. Comparison of the experimental (bold) and theoretically simulated (faint) B 1*s* PhD modulation functions recorded in different emission directions which form the basis of the present structure determination.

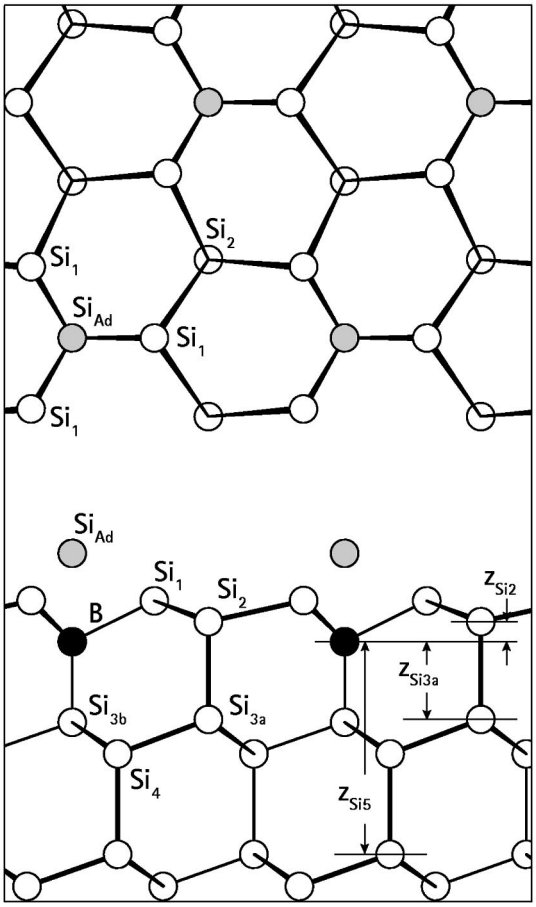

FIG. 4. Plan and sectional views of the Si(111)($\sqrt{3}\times\sqrt{3}$)R30°-B structure as determined in the present study. The labeling conventions for the various Si atoms in the structure are shown, along with the definitions of the various layer spacing parameters. The associated parameter values are listed in Table I.

III. COMPUTATIONAL DETAILS

In most of our recent quantitative structural determinations with scanned energy mode photoelectron diffraction we have adopted a two-stage procedure.[32,33,35,36] In the first stage we use a direct inversion of the experimental data—usually the so-called projection method[39]—to provide a three-dimensional map of the relative positions of scatterer atoms around the emitter atom. This approximate structural solution is then refined by the application of a full quantitative analysis using multiple-scattering simulations on model structures iterated by a ''trial and error'' approach. The present data set was not quite large enough to allow reliable application of the projection method, so that the starting point for the full analysis was the substitutional S_5 adsorption site already determined by x-ray diffraction and LEED, although other possible structures were also investigated. The iterative ''trial and error'' approach consists of comparing the experimental modulation functions (for typically 5–10 different directions) with the results of multiple-scattering simulations based on trial model structures.

These calculations were performed on the basis of an expansion of the final-state wave function into a sum over all scattering pathways which the electron can take from the emitter atom to the detector outside the sample. A magnetic quantum number expansion of the free-electron propagator was used to calculate the scattering contribution of an individual scattering path.[40] Double and higher-order scattering events were treated by means of the reduced angular momentum expansion.[41] The finite-energy resolution and angular acceptance of the electron analyzer are included. Anisotropic vibrations for the emitter atom and isotropic vibrations for the scattering atoms are also taken into account. In an analogous way to LEED the comparison between theory and experiment is aided by the use of a reliability factor, or R factor,

$$R_m = \frac{\sum (\chi_{\rm th} - \chi_{\rm ex})^2}{\sum (\chi_{\rm th}^2 + \chi_{\rm ex}^2)}, \tag{2}$$

where a value of 0 corresponds to perfect agreement, a value of 1 to uncorrelated data, and a value of 2 to anticorrelated data.[33,34] This R factor is specifically designed for photoelectron diffraction where the modulation functions represent a superposition of different oscillatory functions.

The structural parameters optimized were the interatomic distances $d_{\rm Si3b}$, d_{SiAd}, $d_{\rm Si1}$, and $d_{\rm Si4}$, the layer separations $z_{\rm Si2}$, $z_{\rm Si5}$, $z_{\rm Si3a}$, all relative to the B emitter position (see Fig. 4). In addition, the vibrational amplitudes of the emitter

and scatterer atoms were adjusted for the optimum fit. Notice that the PhD technique is sensitive only to the amplitudes of vibration of the scatterer atoms *relative to* the emitter, and not to these individually. For the nearest neighbor scatterers the correlation of the vibrations of the emitter and these nearest neighbors can therefore be important, and the relative mean-square vibrational amplitude derived from the measurements is *not* equal to the sum of the emitter and scatterer vibrations. In order to explore the importance of this effect the mean-square vibrational amplitude of the emitter, $\langle u_{\mathrm{B}}^2\rangle$, was set to zero; the effect of this is that the optimum value of the bulk Si atom mean-square vibrational amplitudes, $\langle u_{\mathrm{Bulk}}^2\rangle$, must be interpreted as actually corresponding to $(\langle u_{\mathrm{B}}^2\rangle+\langle u_{\mathrm{Bulk}}^2\rangle)$ because these two vibrations are uncorrelated. On the other hand, the value derived for the mean-square vibrational amplitude of the nearest neighbors, $\langle u_{\mathrm{SiNear}}^2\rangle$, is really a *relative* vibrational amplitude with respect to the B emitter atom.

The search in parameter space to locate the structure with the minimum R factor was performed with the help of the Marquardt algorithm, in which the calculation of the curvatures is made considerably faster by using the so-called linear method.[42] In order to estimate the errors associated with the individual structural parameters we use an approach based on that of Pendry which was derived for LEED.[43] This involves defining a variance in the minimum of the R factor, $R_{\min}$ as

$$\mathrm{Var}(R_{\min})=R_{\min}\sqrt{\frac{2}{N}}, \tag{3}$$

where N is the number of independent pieces of structural information contained in the set of modulation functions used in the analysis. All parameter values giving structures with R factors less than $R_{\min}+\mathrm{Var}(R_{\min})$ are regarded as falling within one standard deviation of the ''best fit'' structure. More details of this approach, in particular on the definition of N, can be found in a recent publication.[44]

IV. RESULTS AND DISCUSSION

A cursory glance at Fig. 3 (bold curves) shows that the experimental modulation function at normal emission has the largest amplitude modulations and would be approximately cosine-like if it were plotted as a function of the modulus of the photoelectron wave vector, rather than its kinetic energy. Under these experimental conditions the obvious conclusion to be drawn is that a Si atom is situated immediately beneath the emitter, giving rise to the favorable 180° backscattering geometry in which the entrance aperture of the electron energy analyzer, the emitter atom and the backscattering atom are colinear. The modulation function is then dominated by the interference between the directly emitted component of the wave field and the component scattered from this atom due to a maximum in the amplitude of the scattering factor for a scattering angle of 180° in this energy range (e.g., Ref. 32). A similar situation is encountered for a polar emission angle of 41° in the $[1\,2\,\bar{1}]$ azimuth where the modulations are approximately of the same amplitude but their frequency is higher, indicating that the 180° backscattering atom at this angle is further away from the emitter. Both observations are fully compatible with the substitutional S_5 adsorption site found in the previous structural studies.[1,2] The two backscattering atoms are Si_{3b} and Si_4, respectively.

TABLE I. Optimum parameter values for the structural and nonstructural parameters found for $Si(111)(\sqrt{3}\times\sqrt{3})R\,30°$-B. See Fig. 4 for definitions of the Si atom names and layer spacings.

Parameter	Value
Interatomic distances	
d_{Si3b}	1.98(±0.04) Å
d_{Si1}	2.21(±0.13) Å
d_{Si4}	3.53(±0.09) Å
d_{SiAd}	2.14(±0.13) Å
Layer separations	
z_{Si5}	5.20(±0.20) Å
z_{Si2}	0.49(±0.35) Å
z_{Si3a}	1.90(±0.16) Å
Bond angles	
∠(SiAd-B-Si1)	63.5(±2.1)°
∠(SiAd-B-Si4)	141.0(±3.3)°
Vibrational amplitudes	
$\langle u_{\mathrm{SiNear}}^2\rangle$	$0.0005(+0.0056/-0.0005)$ Å^2
$\langle u_{\mathrm{Bulk}}^2\rangle$	$0.006(+0.006/-0.003)$ Å^2
Muffin-tin potential	6.5(±3.5) eV

Using the parameters found by Huang *et al.* in their LEED study[1] as the starting model, we obtained a very poor overall R factor of 0.68. This could be immediately improved to 0.45 by allowing the separation between the B atom and the Si_{3b} atom directly underneath to decrease by 0.15 Å. In the next stage of optimization the positions of the nearest-neighbor atoms Si_{Ad}, Si_{3b} and Si_1 were varied without changing the point-group symmetry of the substitutional site. Using the Marquardt algorithm this gave an R factor of 0.36. In the final stage of the optimization the positions of the next-nearest neighbors Si_4, Si_2, Si_{3a}, and Si_5 were varied, as were the vibrational amplitudes, the effective kinetic energy resolution[45] and value of the average muffin-tin potential.[40] The final R factor obtained was 0.20 with a variance of 0.02. The resulting best-fit modulation functions are shown as gray curves and compared directly with the experimental curves in Fig. 3. The individual R factors (from top to bottom) are 0.11, 0.19, 0.26, 0.18, and 0.45. The agreement for the spectrum recorded at 71° in the $[1\,2\,\bar{1}]$ azimuth is noticeably worse than for the others, but here the modulation amplitude is considerably smaller, so the R factor becomes dominated by discrepancies in weak features. The final optimum values of the structural and nonstructural parameters are given in Table I, while Fig. 4, which shows the associated structure, is drawn such that the relaxation of the Si lattice in the surface region may be compared to the ideally truncated bulk structure of Fig. 1. Notice that the vibrational parameters, despite their limited precision, are consistent with expectations. The uncorrelated sum of the mean-square vibrational amplitudes of the B emitter and the bulk Si atoms is 0.006 Å^2, which is to be compared with an anticipated value for the bulk Si atoms alone based on the Debye temperature of Si of 0.003 Å^2. Evidently the vibrational amplitude of the subsurface substitutional B atoms is similar to

TABLE II. Comparison of some structural parameter values (in Å) obtained in different studies of the Si(111)($\sqrt{3}\times\sqrt{3}$)R 30°-B structure.

	PhD This work	LEED Ref. 3	XRD Ref. 1	Theory (slab) Ref. 4	Theory (cluster) Ref. 5
d_{Si3b}	1.98($\pm$0.04)	2.19($\pm$0.14)	2.00[a]	2.04	1.97
d_{Si1}	2.21($\pm$0.13)	2.15($\pm$0.18)	2.18($\pm$0.09)	2.14	2.12
d_{SiAd}	2.14($\pm$0.13)	2.32($\pm$0.14)	1.98($\pm$0.2)	2.22	2.20

[a]In this reference they assumed a constrained value of this distance.

that of the bulk Si atoms. By contrast, the relative mean-square vibrational amplitude of the near-neighbor Si atoms with respect to the B emitter is much smaller, indicating strong correlations in these vibrations.

To be certain that the result really corresponded to a global minimum of the R factor in the multiparameter space investigated, an additional systematic grid search was also performed using the linear method.[42] No further minima with anything like the depth of the one established could be found. Additionally, two other, completely different models were checked; in the first the boron atom was left in the S_5 site but the Si adatom was removed, while in the second the boron atom occupied the T_4 site. After full optimization R factors of 0.27 and 0.46 were obtained for these two structures. Note that although the first of these structures without the adatom leads to a comparatively low R factor, its value is well above that of the minimum R factor plus its variance (0.22) corresponding to the structure obtained above. Various mixtures of all three structures in different ratios were also tried, but did not produce a better R factor. We therefore conclude that the global minimum had been found. Table II shows a comparison of the near-neighbor B-Si distances obtained in this work and from previous experimental and theoretical studies. The only other experimental investigation providing a complete set of such parameters is the LEED investigation[3] and clearly has a significantly lower precision (we have estimated the precision in these bond lengths from the cited errors estimates for individual atomic positions). Because of the large error estimates the two experimental data sets are formally consistent with one another, and indeed with almost all the theoretically derived values. The best-fit values in our study for the distances to the Si atoms directly above (d_{SiAd}) and below (d_{Si3b}) the B atoms, however, are significantly closer to the theoretical values than are the best-fit LEED values; in view of the improved precision, our results therefore substantially support the results of the theoretical total-energy calculations, slightly favoring the results of the cluster calculations of Wang *et al.*[5]

V. CONCLUSIONS

Although there has for some time been a consensus, based on both experimental and theoretical studies, that the Si(111)($\sqrt{3}\times\sqrt{3}$)R 30°-B structure is unusual in having the adsorbate B atom in a subsurface S_5 site, the only quantitative experimental determination of the local geometry of the B atom, achieved in a LEED study[3] had rather limited precision. The low atomic number B atom is problematic in both x-ray and electron diffraction due to its small scattering cross section. Here we have applied the technique of scanned-energy mode photoelectron diffraction to this problem, using the B atom as the source of the electrons to be scattered and thus circumventing this problem. The use of the high spectral brilliance synchrotron radiation from a third-generation source (ALS) allows us to overcome the problems created by the low photoionization cross section of the B 1s core level. The results confirm the occupation of the S_5 site by the B atoms, but also provide relatively precise values for the B-Si nearest-neighbor distances which agree well with the results of theoretical total-energy calculations published previously.

ACKNOWLEDGMENTS

The authors are pleased to acknowledge financial support from the Federal Ministry for Education, Science, Research, and Technology (Germany) under Contract Nos. 05 SF8EBA 4 and 05 622OLA 3, the Deutsche Forschungsgemeinschaft (Pa661/1-1), as well as the Physical Sciences and Engineering Research Council (U.K.). They also gratefully acknowledge the award of beamtime at the Advanced Light Source (ALS) which is supported by the Office of Energy Research, Office of Basic Energy Science, Materials Science Division of the U.S. Department of Energy under Contract No. DE-AC03-76SF00098. A.M.B. and D.P.W. thank the Humboldt Foundation and the Max Planck Society for financial support.

*Permanent address: Department of Chemical Engineering and Materials Science, University of Minnesota, Minneapolis, MN 55455.

[1] R. L. Headrick, I. K. Robinson, E. Vlieg, and L. C. Feldman, Phys. Rev. Lett. **63**, 1253 (1989).

[2] K. Akimoto, I. Hirsawa, T. Tatsumi, H. Hirayama, J. Mizuki, and J. Matsui, Appl. Phys. Lett. **56**, 1225 (1990).

[3] H. Huang, S. Y. Tong, J. Quinn, and F. Jona, Phys. Rev. B **41**, 3276 (1990).

[4] I.-W. Lyo, E. Kaxiras, and Ph. Avouris, Phys. Rev. Lett. **63**, 1261 (1989).

[5] Sanwu Wang, M. W. Radny, and P. V. Smith, Surf. Sci. **394**, 235 (1997).

[6] T.-C. Shen, C. Wang, J. W. Lyding, and J. R. Tucker, Phys. Rev. B **50**, 7453 (1994).

[7] A. V. Zotov, M. A. Kulakov, S. V. Ryzhkov, A. A. Saranin, V. G. Lifshits, B. Bullemer, and I. Eisele, Surf. Sci. **345**, 313 (1996).

[8] J. T. Yates, Jr., J. Phys.: Condens. Matter **3**, S143 (1991).

[9] P. J. Chen, M. L. Colaianni, and J. T. Yates, J. Appl. Phys. **70**, 2954 (1991).
[10] Y. Ma, J. E. Rowe, E. E. Chaban, C. T. Chen, R. L. Headrick, G. M. Meigs, S. Modesti, and F. Sette, Phys. Rev. Lett. **65**, 2173 (1990).
[11] F. Bozso and Ph. Avouris, Phys. Rev. B **44**, 9129 (1991).
[12] Y. Ma, C. T. Chen, G. Meigs, F. Sette, G. Illing, and H. Shigakawa, Phys. Rev. B **45**, 5961 (1992).
[13] Ph. Mathiez, T. P. Roge, Ph. Dumas, and F. Salvan, Appl. Surf. Sci. **56-58**, 551 (1992).
[14] B. Müller, O. Jusko, G. J. Pietsch, and U. Köhler, J. Vac. Sci. Technol. B **10**, 16 (1992).
[15] H. H. Weitering, J. Chen, N. J. DiNardo, and E. W. Plummer, Phys. Rev. B **48**, 8119 (1993).
[16] H. H. Weitering, J. Chen, N. J. DiNardo, and E. W. Plummer, J. Vac. Sci. Technol. A **11**, 2049 (1993).
[17] Y. Taguchi, M. Daté, N. Takagi, T. Aruga, and M. Nishijima, Phys. Rev. B **50**, 17440 (1994).
[18] Y. Taguchi, M. Daté, N. Takagi, T. Aruga, and M. Nishijima, Appl. Surf. Sci. **82/83**, 434 (1994).
[19] H. H. Weitering, J. Chen, R. Perez-Sandoz, and N. J. DiNardo, Surf. Sci. **307-309**, 978 (1994).
[20] T. M. Grehk, M. Gthelid, U. O. Karlsson, L. S. O. Johanson, S. M. Gray, and K. O. Magnusson, Phys. Rev. B **52**, 11 165 (1995).
[21] R. L. Headrick, L. C. Feldman, and I. K. Robinson, Appl. Phys. Lett. **55**, 442 (1989).
[22] R. L. Headrick, B. E. Weir, J. Bevk, B. S. Freer, D. J. Eaglesham, and L. C. Feldmann, Phys. Rev. Lett. **65**, 1128 (1990).
[23] R. L. Headrick, B. E. Weir, A. F. J. Levi, B. Freer, J. Bevk, and L. C. Feldman, J. Vac. Sci. Technol. A **9**, 2269 (1991).
[24] R. L. Headrick, A. F. J. Levi, H. S. Luftman, J. Kovalchick, and L. C. Feldman, Phys. Rev. B **43**, 14 711 (1991).
[25] A. V. Zotov, M. A. Kulakov, S. V. Ryzhkov, V. G. Lifshits, B. Bullemer, and I. Eisele, Surf. Sci. **352-354**, 358 (1996).
[26] A. V. Zotov, M. A. Kulakov, B. Bullemer, and I. Eisele, Phys. Rev. B **53**, 12 902 (1996).
[27] T. Tatsumi, I. Hirosawa, T. Niino, H. Hirayama, and J. Mizuki, Appl. Phys. Lett. **57**, 73 (1990).
[28] A. B. McLean, L. J. Terminello, and F. J. Himpsel, Phys. Rev. B **41**, 7694 (1990).
[29] J. E. Rowe, G. K. Wertheim, and D. M. Riffe, J. Vac. Sci. Technol. A **9**, 1020 (1991).
[30] R. Cao, X. Yang, and P. Pianetta, J. Vac. Sci. Technol. A **11**, 1817 (1993).
[31] J. Chang and M. J. Stott, Phys. Status Solidi B **200**, 481 (1997).
[32] D. P. Woodruff and A. M. Bradshaw, Rep. Prog. Phys. **57**, 1029 (1994).
[33] Ph. Hoffmann, K.-M. Schindler, S. Bao, V. Fritzsche, A. M. Bradshaw, and D. P. Woodruff, Surf. Sci. **337**, 169 (1995).
[34] R. Dippel, K.-U. Weiss, K.-M. Schindler, D. P. Woodruff, P. Gardner, V. Fritzsche, A. M. Bradshaw, and M. C. Asensio, Surf. Sci. **287/288**, 465 (1993).
[35] D. P. Woodruff, R. Davis, N. A. Booth, A. M. Bradshaw, C. J. Hirschmugl, K-M. Schindler, O. Schaff, V. Fernandez, A. Theobald, Ph. Hofmann, and V. Fritzsche, Surf. Sci. **357/358**, 19 (1996).
[36] N. A. Booth, D. P. Woodruff, O. Schaff, T. Giessel, R. Lindsay, P. Baumgärtel, and A. M. Bradshaw, Surf. Sci. **397**, 258 (1998).
[37] T. Warwick, P. Heimann, D. Mossessian, W. McKinney, and H. Padmore, Rev. Sci. Instrum. **66(2)**, 2237 (1995).
[38] T. Warwick, M. Howells, and M. Shlezinger, Rev. Sci. Instrum. **66(2)**, 2270 (1995).
[39] Ph. Hofman and K.-M. Schindler, Phys. Rev. B **47**, 13 941 (1993); Ph. Hofmann, K.-M. Schindler, S. Bao, A. M. Bradshaw, and D. P. Woodruff, Nature (London) **368**, 131 (1994).
[40] V. Fritzsche, J. Phys.: Condens. Matter **2**, 1413 (1990); Surf. Sci. **256**, 187 (1992).
[41] V. Fritzsche, Surf. Sci. **213**, 648 (1986).
[42] V. Fritzsche and J. B. Pendry, Phys. Rev. B **48**, 9054 (1993).
[43] J. B. Pendry, J. Phys. C **13**, 937 (1980).
[44] N. A. Booth, R. Davis, R. Toomes, D. P. Woodruff, C. Hirschmugl, K. M. Schindler, O. Schaff, V. Fernandez, A. Theobald, Ph. Hofmann, R. Lindsay, T. Giessel, P. Baumgärtel, and A. M. Bradshaw, Surf. Sci. **387**, 152 (1997).
[45] V. Fritzsche, Surf. Sci. **265**, 187 (1992).